NON-SULFURIZATION SINGLE SOLUTION APPROACH TO SYNTHESIZE CZTS THIN FILMS

Badrul Munir[1], Bayu Eko Prastyo[1*], Ersan Yudhapratama Muslih[2], Dwi Marta Nurjaya[1]

[1]*Department of Metallurgy and Materials Engineering, Faculty of Engineering, Universitas Indonesia Kampus UI Depok, Depok 16424, Indonesia*
[2]*Department of Mechanical Engineering, Faculty of Engineering, Trisakti University, Jakarta 11440, Indonesia*

ABSTRACT

The growth and crystallization processes of the Cu_2ZnSnS_4 (CZTS) phase typically rely on high-temperature sulfurization, which involves a harmful chalcogen-containing atmosphere. Together with the use of high-toxicity solvents, these processes could hinder the widespread adoption of this technology in the mass production of CZTS semiconductors for solar cell application. Thus, we studied the formation of CZTS films from ethanol-based precursors without the sulfurization step, fully employing the non-toxic solvent and avoiding the environmentally harmful sulfur-containing atmosphere. The certain addition of 2-mercaptopropionic acid led to the formation of a clear and stable sulfur-containing precursor. The precursors were successfully deposited onto soda lime glass by employing spin coater. CZTS crystallinity in the identified XRD patterns was vanishingly small in the case of eliminating the sulfurization process. Moreover, the carbon concentration and grain size of the resulting films were controlled by changing the time period of drying treatment during film fabrication. A drying time of 120 minutes, which demonstrated a CZTS grain size of ± 1 µm with a direct optical energy gap around 1.4 eV, was confirmed as the ideal condition. These results may provide a useful route toward environment-friendly strategies for the production of a CZTS semiconductor that is compatible with the absorber application in thin-film solar cells.

Keywords: Cu_2ZnSnS_4 semiconductor; Drying treatment; Sulfurization; Sulfur-containing precursor; Thin-film solar cells

1. INTRODUCTION

The Cu_2ZnSnS_4 (CZTS) semiconductor has emerged as a new type of potential absorber material for the large scale production of solar cells. This quaternary chalcogenide p-type semiconductor consists of non-toxic and high earth abundant elements. Its tunable direct optical energy gap (˜1.0–1.5 eV) and high absorption coefficient of ˜10^4 cm^{-1} have attracted the thin-film solar cell (TFSCs) application (Larramona et al., 2014; Persson, 2010). TFSC is the second generation of solar technology in the order of converting solar radiation into electricity by employing certain direct band gap material to obtain a remarkably thin and low cost device. TFSC, itself, is continuously growing and has reduced the use of standard crystalline silicon solar devices for commercial application.

Various types of absorber material have been developed since material is the main issue affecting the

performance of solar cells. Meanwhile, supporting layers such as the n-type semiconductor, emitter layer and charge collector have also been evaluated for commercial application. Currently, commercial TFSC technology is dominated by cadmium telluride (CdTe) and $CuIn_xGa_{(1-x)}Se_2$ (CIGS) as p-type semiconductors (Parida et al., 2011). CdTe is superior in the relatively simple production process, while CIGS is excellent regarding power-conversion efficiency (PCE). The best PCE for laboratory cells has been reported as high as 18.3% and 20.3%, respectively, for CdTe and CIGS (Gessert et al., 2013; Jackson et al., 2014). Recently, CZTS has been approaching its predecessor semiconductors, with a PCE 12.6%, which is a huge improvement (Green et al., 2013). CZTS is, therefore, attractive for the terra watt production scale of its solar cells since CdTe and CIGS are limited by the high toxicity and scarcity of their elemental components.
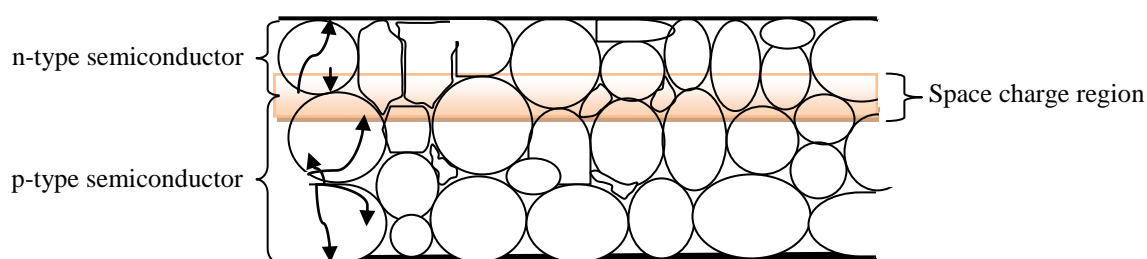

Figure 1 Schematic overview of charge carriers' movement through p-type and n-type junctions

The wet-chemical route of preparing CZTS precursors offers an excellent opportunity for commercial use due to its versatility to be used in a wide range of deposition processes, such as printing techniques, spray pyrolisis, doctor blade and spin coating. To date, high-performance CZTS solar cells are those made from high temperature annealing under a chalcogen atmosphere (sulfurization and selenization) and/or with hydrazine molecular-based precursors (Liu et al., 2015). Hydrazine is a flammable and high-toxicity solvent. Together with chalcogen atmosphere, both routes need exclusive and expensive protocols. However, the highest efficiency of CZTS-based solar cells has been obtained using hydrazine methodologies (Mitzi et al., 2011; Wang et al., 2014). Hydrazine approaches permit the formation of high purity CZTS or CZTSSe (incorporation of selenium) phases and provide relatively easy control in chemical composition. Recent scientific efforts in the CZTS research group have been focused on developing a new route to address the formation of secondary phases, obtain a CZTS phase with high crystallinity and avoid the use of toxic solvents. The results presented herein present new strategies for the fabrication of a CZTS semiconductor from non-toxic solvent ethanol without a sulfurization process.

Careful selection of precursors and thermal treatment is essential to support the photo-conversion performance of the device, which occurs inside the semiconductor layer (p-type and n-type). The p-type semiconductor has a high concentration of holes and, thus, is so-called the positively charged layer; whereas, the n-type semiconductor has a high concentration of electrons and, thus, is so-called the negatively charged layer. The space charge region, or the area of built-in field formed due to the diffusion movement of electrons and holes (so-called electron-hole pairs), is triggered by the gradient concentration between the semiconductor junctions. Afterwards, the built-in field induces the drift movement of electrons and holes in opposite directions and forms the area of equilibrium, as shown in Figure 1. Electron-hole pairs are charge carriers that form inside of the semiconductor junction, mainly induced by photon energy from solar radiation. From the formation of supporting layers, such as the emitter layer, charge collectors and intrinsic layer, the charges will be converted into electricity. Defects,

porosity and unlinear lattice orientation serve the energy state for charge carriers to recombine back to the neutral state. It is, therefore, important to control grain size, cristallinity and defects, as well as carbon concentration, inside the semiconductor. Carbon concentration is of particular interest in this report since carbon has low electric conductivity. By designing the time period of the drying treatment, we not only controlled the carbon concentration inside the CZTS semiconductor but also observed the grain size and crystallinity of the CZTS phase.

2. EXPERIMENTAL SETUP

2.1. Materials

The chemicals copper chloride ($CuCl_2$), zinc chloride ($ZnCl_2$), tin chloride ($SnCl_2$), thiourea and 2-mercaptopropionic acid were purchased from Across Organic and used directly as received. The main solvent, ethanol, was obtained from Merck. Acetone and distilled water, which were used as the chemicals for substrate preparation, were commercially obtained from a local producer.

2.2. Precursors Synthesis and Film Deposition

The chemical compositions Cu-poor (Cu/(Sn+Zn): 0.8 and Zn rich (Zn/Sn): 1.2 were used as references in preparing the CZTS precursors. For the typical experiment, 16 mmol $CuCl_2$, 9 mmol $SnCl_2$ and 10.9 mmol $ZnCl_2$ were completely dissolved in 16.5 ml ethanol with the addition of 1.5 ml 2-mercaptopropionic acid. The solution was heated up to 160 ^{o}C and kept for 15 min with stirring. Afterwards, 80 mmol thiourea was hot injected into the solution and kept for another 5 min. at the same temperature with stirring. The experimental pictures associated with the typical experimental are shown in Figure 2.
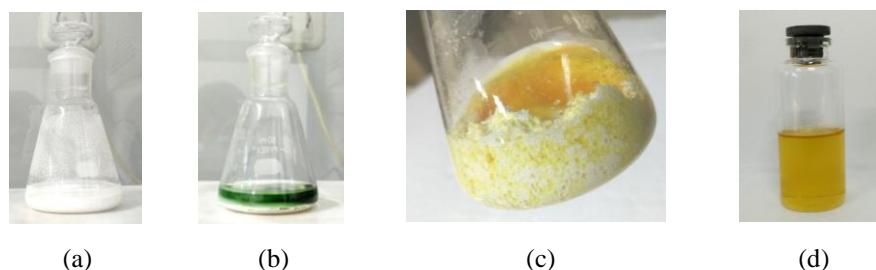

(a) (b) (c) (d)

Figure 2 Experimental pictures of: (a) ethanol solution of Cu-Zn-Sn; (b) addition of 2-mercaptopropionic acid; (c) addition of thiourea; and (d) final CZTS precursor

Prior to fabricating CZTS films, soda lime glass was used as a substrate. Before the deposition process, substrates were baked into acetone, ethanol and distilled water using ultrasonic cleaner for 10 min., respectively. Finally, the CZTS precursors were spun onto the substrate at 2500 rpm for 20 s., followed by the drying process at 170°C for 10 min. These cycles were repeated three times to obtain a thick CZTS film. In order to control carbon concentration, different drying time periods were conducted during the final cycle in the order of 30, 90 and 120 min. The influences of drying period on the grain size, carbon concentration and chemical composition at the final films are recorded.

2.3. CZTS-phase Growth

To investigate the growth process of the CZTS phase and the role of the sulfur containing-precursor, two different annealing atmospheres were executed. The first annealing was conducted in a fully-argon atmosphere, and the second annealing was conducted in a sulfur-containing atmosphere (argon was still employed to prevent the involvement of oxygen). Both annealings were conducted at a holding temperature of 540°C for 30 minutes.

3.   RESULTS AND DISCUSSION

Sulfurization or annealing in a sulfur-containing atmosphere is predominantly used as the common approach in the fabrication of CZTS semiconductors. Initial precursors of Cu-Zn-Sn are deposited onto certain substrates, and incorporations of sulfur occur during the sulfurization step before the finally formed Cu-Zn-Sn-S compound. Other researches have even employed the sulfurization step in the use of Cu-Zn-Sn-S nanoparticle deposition (Thimsen et al., 2012). In contrast, we developed sulfur-containing precursors at a certain excess sulfur fraction in order to eliminate the sulfurization step. The selection of the excess sulfur fraction was particularly important since thiourea, which is used as a sulfur source, melts at 176°C, while pure sulfur itself melts at 116°C. It is, therefore, rather tricky in the co-optimization process since the growth of the CZTS phase requires high temperature annealing in the order of 500°C.

Regarding the sensitivity of the precursor system to the result of fabricating $\pm$ 2µm thick CZTS film, over 60 combinations were tried by designing the selection of solvents and capping ligand, as well as the volume fraction of each chemical and mol fraction of the sulfur source. The addition of 2-mercaptopropionic acid to the ethanol-based CZTS precursor was found as the ideal condition to obtain a clear and homogenous precursor. The precursors were succesfully deposited onto soda lime glass with strong adhesive force. At the initial precursor, the sulfur content kept the unstoichiometry excess and finally fixed at the number of 5 times the mol of Cu. Next, we prepared three samples without modification in the final drying treatment and exclusively investigated the role of the excess sulfur-containing precursor to the generation of the CZTS phase in the absence of sulfurization. Figure 3 shows the XRD patterns of the three samples: the sample before annealing and the annealed samples with and without sulfurization. Note that each sample was prepared from sulfur-containing precursors.
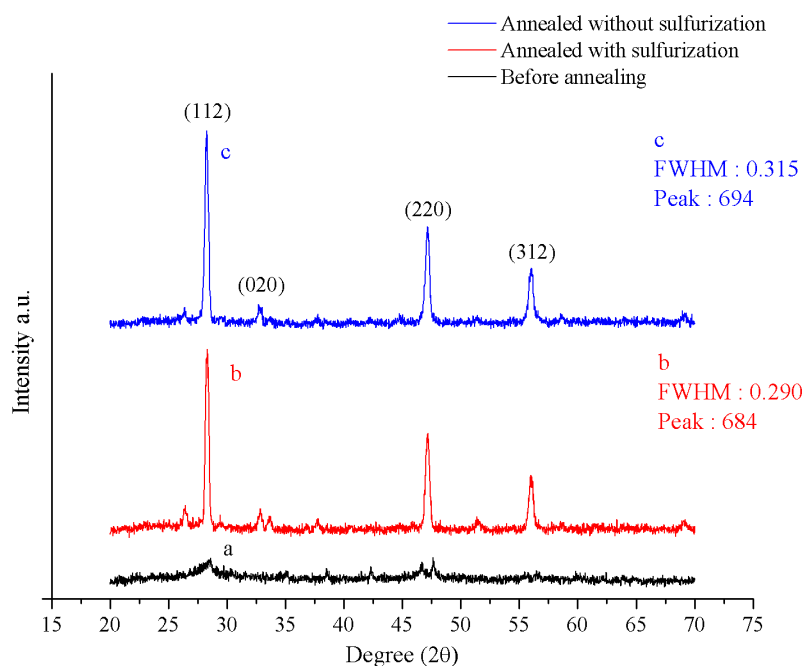

Figure 3 XRD patterns of: (a) as-deposited CZTS film; (b) annealed with sulfurization; and (c) annealed without sulfurization

The XRD patterns (Figure 3) exhibited intense peaks for tetragonal CZTS, along with less intense peaks for secondary phases ZnS and CuS_x. We can observe the importance of the annealing process for CZTS growth by considering the significant rise of typical CZTS peaks

before and after annealing. The comparison in Figure 3 shows decreases of CZTS intense peaks by using the dangerous sulfurization process. These observations give a preliminary indication that the precursors are suitable for generating a high quality CZTS semiconductor without sulfurization.

To develop this idea, we realized that the case of adding more thiourea (CH_4N_2S) results in higher concentration of carbon in the precursors. Carbon concentration can negatively affect solar cell performance, reduce electric conductivity, increase recombination process and short circuit. In order to reduce carbon concentration, designing time period and temperature of drying treatment were performed. The temperature is selected in between above boiling point of solvent as well as capping ligand and below the melting point of elemental constituents of CZTS. The employment of 2-mercaptopropionic acid is remarkable protrude since it has low boiling point and confidently formed complex binary sulphides compound.
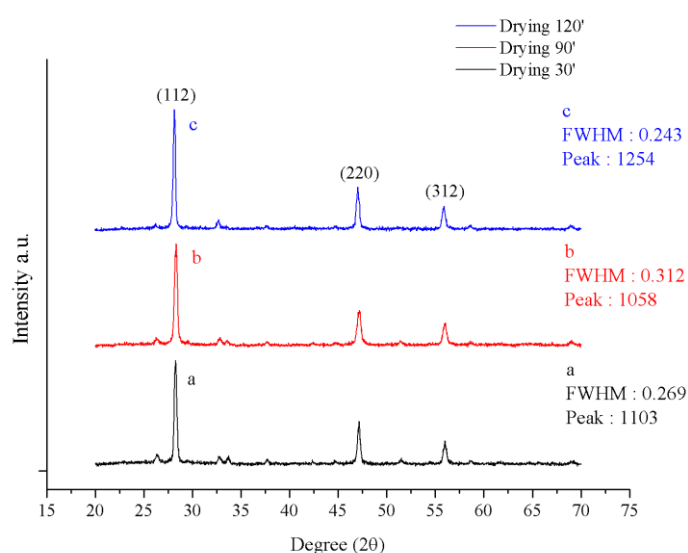

Figure 4 XRD patterns of CZTS film exposed to: (a) 30; (b) 60; and (c) 90 minutes of drying treatment

Figure 4 shows the XRD pattern of samples exposed to different period of drying treatment. The patterns can be assigned to be kesterite CZTS phase based on ICDD Ref. No. 00-026-0575, particularly in the orientation of (112), (220) and (312). Sample exposed to 120 min. showed relatively clear pattern and has the highest crystallinity (peak). In addition, the sample has the lowest carbon concentration and narrow FWHM (Full Width at Half Maximum). Tan et al. (2014) have confirmed the sequence process to generate CZTS phase; firstly induced nucleation of $Cu_{2-x}S$, followed by the diffusion of Sn^{4+} to form Cu_3SnS_4 (CTS) and finally involved solid state diffusion of Zn^{2+} to form CZTS. Consequently, direct contact of each sulphides compound is strongly influence the kinetics of solid state diffusion. Carbon behave as secondary arbiter element, thus impedes the formation of CZTS phase. The carbon concentration and other chemical composition are listed in Table 1.

Table 1 Chemical composition of final CZTS films

Samples	Drying period (min)	%wt of C	Cu/(Zn+Sn)	Zn/Sn	S/metal
D 60	30	10.91	0.90	0.71	0.87
D 90	90	9.70	0.86	1.30	0.93
D 120	120	7.86	0.68	1.28	0.96

Cu poor and Zn rich are the conditions when Cu/(Zn+Sn) < 1 and Zn/Sn > 1, respectively in mol fraction. As the prime prerequisites for generating charge carriers by chemical inequilibrium, these condition have been proved in the fabrication of high-performance CZTS-based solar cells (Choubrac et al., 2012). Most of them reported to have Cu poor and Zn rich in the values of 0.8 and 1.22, respectively (Hiroi et al., 2014; Lee et al., 2015). Table 1 presents the conditions of Cu poor and Zn rich in each sample. It is well understood that, through thermal treatment, final composition will strongly depend on the melting point of each constituent. Table 1 shows relatively broad variations of Cu poor and Zn rich values due to the kinetic reactions that form particles and final compounds. For instance, the reaction step in generating CTS occurs below 200°C, and this compound has melting temperature over 600°C (Tan et al., 2014). Other sulphide binary compounds will also form during final phase CZTS formation. These compound have melting point that are distinguishable from their constituents. Based on previous explanation about the influence of carbon content on CZTS phase formation, these varying are not surprising.

The carbon content dependently correlated to the selection of solvent, capping ligand and chemical composition at the initial precursor. Fortunately, the content can be removed through thermal treatment and could be optimized by employing certain atmospheres which have high affinity to carbon. When carbon decomposes to form gaseous phases, these gases will leaving pathway inside the films before, finally free, arriving at the surface. This mechanism affects the morphology and grain size of CZTS phase. Figure 5 shows images of the surface morphology of the CZTS films.
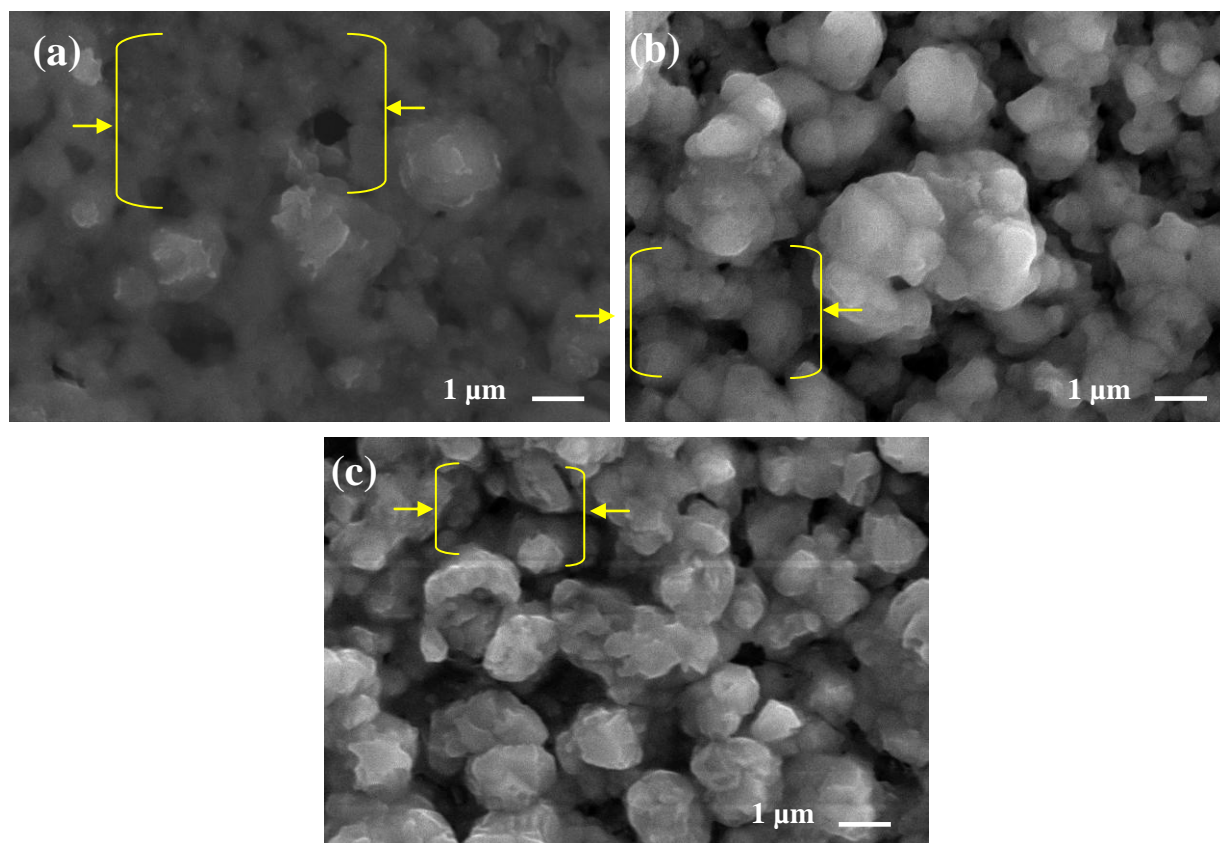

Figure 5 SEM micrographs of the surface morphology of CZTS film exposed to: (a) 30; (b) 60; and (c) 90 minutes of drying treatment

Constraints on morphology are especially challenging in solar device fabrication. Photo-generated charge carriers need a crystalline phase, a homogenous grain size and vanishingly

small defects and porosity to effectively move through the lattice crystal of the device, allowing for the enhancement of solar cell performance. Figure 5 shows the influence of carbon concentration on the morphology and grain size. Prolonged drying treatment established the time for carbon and organic chemicals to decompose and form a gaseous phase and thus form porosity inside the semiconductor. The challenge was controlling CZTS growth to compensate the porosity and, finally, obtain densed morphology. Since the CZTS growth occurred during the annealing process, we can prescribe that annealing performed in this research does not satisfy the kinetics of CZTS growth to recover the porosity. On the basis of this model, prolonging the annealing process should yield the smooth morphology of the final films.

Abou-Ras et al. (2008) found the dependence of thin-film solar cell efficiency on the grain size. High-efficiency of these device has been found for grain sizes around 1 μm. Grain boundaries, together with porosity, are expected to cause potential barriers, as well as increased recombination of charge carriers, because of the high density of broken and unlinear crystal orientation.
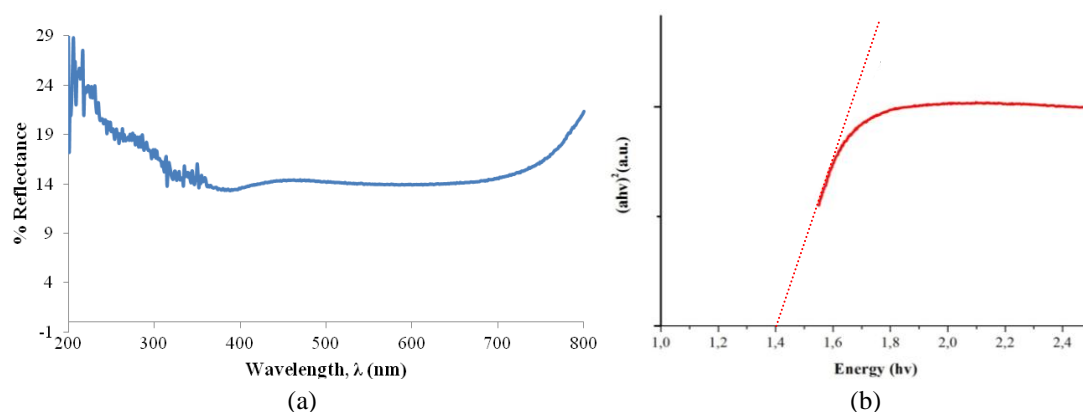

Figure 6 Optical properties of CZTS films, e.g.: (a) Reflectance graph; and (b) Tauc's relation, $(\alpha h\upsilon)^2$ vs hυ, to determine optical energy gap

Further observation was that optical energy gap, which deduced from optical characteristics (transmittance and reflectance) of the films. The film exposed to 120 min. of drying treatment is chosen as the sample since it demonstrated positive crystallinity, the lowest carbon concentration and relatively smooth morphology. Transmittance and reflectance were measured using UV Vis spectroscopy. The optical energy gap (Eg) was determined by performing Tauc's plot from the linear extrapolation of $(\alpha h\upsilon)^2$ versus hυ based on the UV Vis measurements. Figure 6 shows the graphs of (%) reflectance and $(\alpha h\upsilon)^2$ versus hυ (optical energy gap). The fall of reflectance, which occurred in the spectral range of 400–700 nm, indicated the optimum absorption of CZTS film along that wavelength. This range is preferred in the application of solar cells since the optimum spectrum for solar radiation is in the order of 550 nm. After plotting $(\alpha h\upsilon)^2$ versus photon energy (hυ), the optical energy gap for the film was found to be 1.4 eV (Figure 6b). This number is positively supported by another research on the fabrication of CZTS semiconductor. Figure 6b shows uncompleted plot of $(\alpha h\upsilon)^2$ vs hυ along the full spectrum of real sun radiation, but it has sufficient to deduce the optical energy gap of the film.

4.   CONCLUSION

The sulfur-containing precursor, with 2-mercaptopropionic acid as a capping ligand, has been shown to induce a high crystallinity CZTS phase without the sulfurization process. Carbon impurity inside the CZTS film, as a result of employing the excess sulfur source, can be

minimized by prolonging the time period of drying treatment. The morphology was found to be affected by the decomposition of the organic compound during drying treatment. CZTS film exposed to 120 min. of drying treatment was found to form a homogenous grain size around 1 μm with a low concentration of carbon impurity. Despite this, the film still had detrimental porosity, which affects the photo-conversion performance of solar cells. The observation of the CZTS phase growth mechanism suggests establishing sufficient time for CZTS grain growth to compensate the porosity. This study holds the potential to achieve a high crystalline CZTS semiconductor without introducing the harmful sulfurization process, which is expected to become an alternative route in the fabrication of CZTS-based solar cells.

5.　ACKNOWLEDGEMENT

6.　REFERENCES

Abou-Ras, D., Caballero, R., Kaufman, C.A., Nichterwitz, M., Sakurai, K., Schorr, S., Unold, T., Schock, H.W., 2008. Impact of the Ga Concentration on the Microstructure of $CuIn_{1-x}Ga_xSe_2$. *Physica Status Solidi-Rapid Research Letters*, Volume 2(3), pp. 135–137

Choubrac, L., Lafond, A., Guillot-Deudon, C., Moëlo, Y., Jobic, S., 2012. Structure Flexibility of the Cu_2ZnSnS_4 Absorber in Low-cost Photovoltaic Cells: From the Stoichiometric to the Copper-poor Compounds. *Inorganic Chemistry*, Volume 51(6), pp. 3346−3348

Gessert, T.A., Wei, S.-H., Ma, J., Albin, D.S., Dhere, R.G., Duenow, J.N., Kuciauskas, D., Kanevce, A., Barnes, T.M., Burst, J.M., Rance, W.L., Reese, M.O., Moutinho, H.R., 2013. Research Strategies toward Improving Thin-film CdTe Photovoltaic Devices Beyond 20% Conversion Efficiency. *Solar Energy Materials and Solar Cells*, Volume 119, pp. 149–155

Green, M.A., Emery, K., Hishikawa, Y., Warta, W., Dunlop, E.D., 2013. Solar Cell Efficiency Tables (Version 41). *Progress in Photovoltaics: Research and Applications*, Volume 21(1), pp. 1–11

Hiroi, H., Kim, J., Kuwahara, M., Todorov, T.K., Nair, D., Hopstaken, M., Zhu, Y., Gunawan, O., Mitzi, D.B., Sugimoto, H., 2014. Over 12% Efficiency $Cu_2ZnSn(SeS)_4$ Solar Cell via Hybrid Buffer Layer. *In*: Proceedings of the 40th IEEE Photovoltaic Specialists Conference, At Denver, Colorado, USA, Volume 30-32, pp. 30–32

Jackson, P., Hariskos, D., Wuerz, R., Kiowski, O., Bauer, A., Friedlmeier, T.M., Powalla, M., 2014. Properties of $Cu(In,Ga)Se_2$ with New Record Efficiencies up to 21.7%. *Physica Status Solidi-Rapid Research Letters*, Volume 9(1), pp. 28−31

Larramona, G., Bourdais, S., Jacob, A., Choné, C., Muto, T., Cuccaro, Y., Delatouche, B., Moisan, C., Péré, D., Dennler, G., 2014. 8.6% Efficient CZTSSe Solar Cells Sprayed from Water−Ethanol CZTS Colloidal Solutions. *Journal of Physical Chemistry Letters*, Volume 5(21), pp. 3763−3767

Lee, Y.S., Gershon, T., Gunawan, O., Todorov, T.K., Gokmen, T., Virgus, Y., Guha, S., 2015. $Cu_2ZnSnSe_4$ Thin-Film Solar Cells by Thermal Co-evaporation with 11.6% Efficiency and Improved Minority Carrier Diffusion Length. *Advanced Energy Materials*, Volume 5(7), pp. 14013721−14013724

Liu, F., Zeng, F., Song, N., Jiang, L., Han, Z., Su, Z., Yan, C., Wen, X., Hao, X., Liu, Y., 2015. Kesterite $Cu_2ZnSn(S,Se)_4$ Solar Cells with Beyond 8% Efficiency by a Sol-gel and Selenization Process. *ACS Applied Materials & Interfaces*, Volume 7(26), pp. 14376–14383

Mitzi, D.B., Gunawan, O., Todorov, T.K., Wang, K., Guha, S., 2011. The Path towards a High-performance Solution-processed Kesterite Solar Cell. *Solar Energy Materials and Solar Cells*, Volume 95(6), pp. 1421–1436

Parida, B., Iniyan, S., Goic, R., 2011. A Review of Solar Photovoltaic Technologies. *Renewable and Sustainable Energy Reviews*, Volume 15(3), pp. 1625−1636

Persson, C., 2010. Electronic and Optical Properties of Cu_2ZnSnS_4 and $Cu_2ZnSnSe_4$. *Journal of Applied Physics*, Volume 107(5), pp. 0537101−0537108

Tan, J.M.R., Lee, Y.H., Pedireddy, S., Baikie, T., Ling, W.Y., Wong, L.H., 2014. Understanding the Synthetic Pathway of a Single-Phase Quarternary Semiconductor Using Surface-Enhanced Raman Scattering: A Case of Wurtzite Cu_2ZnSnS_4 Nanoparticles. *Journal of the American Chemical Society*, Volume 136(18), pp. 6684−6692

Thimsen, E., Riha, S.C., Baryshev, S.V., Martinson, A.B.F., Elam, J.W., Pellin, M.J.., 2012. Atomic Layer Deposition of the Quaternary Chalcogenide Cu_2ZnSnS_4. *Chemistry of Materials*, Volume 24(16), pp. 3188−3196

Wang, W., Winkler, M.T., Gunawan, O., Gokmen, T., Todorov, T.K., Zhu, Y., Mitzi, D.B, 2014. Device Characteristics of CZTSSe Thin-Film Solar Cells with 12.6% Efficiency. *Advanced Energy Materials*, Volume 4(7), pp. 13014651−13014655